



HAL
open science

Low-Density Plastic Debris Dispersion beneath the Mediterranean Sea Surface

Alberto Baudena, Rainer Kiko, Isabel Jalón-Rojas, Maria Luiza Pedrotti

► **To cite this version:**

Alberto Baudena, Rainer Kiko, Isabel Jalón-Rojas, Maria Luiza Pedrotti. Low-Density Plastic Debris Dispersion beneath the Mediterranean Sea Surface. *Environmental Science and Technology*, 2023, 10.1021/acs.est.2c08873 . hal-04087301

HAL Id: hal-04087301

<https://hal.sorbonne-universite.fr/hal-04087301>

Submitted on 10 May 2023

HAL is a multi-disciplinary open access archive for the deposit and dissemination of scientific research documents, whether they are published or not. The documents may come from teaching and research institutions in France or abroad, or from public or private research centers.

L'archive ouverte pluridisciplinaire **HAL**, est destinée au dépôt et à la diffusion de documents scientifiques de niveau recherche, publiés ou non, émanant des établissements d'enseignement et de recherche français ou étrangers, des laboratoires publics ou privés.

Copyright

1 *Low-density plastic debris dispersion beneath*
2 *the Mediterranean Sea surface*

3 Alberto Baudena^{1,*} Rainer Kiko^{1,2} Isabel Jalón-Rojas³
4 Maria Luiza Pedrotti ¹

5 ¹Sorbonne Université, CNRS, Laboratoire d’Océanographie de Villefranche,
6 UMR 7093 LOV, Villefranche-sur-Mer, France

7 ² GEOMAR Helmholtz Center for Ocean Research Kiel, Germany

8 ³CNRS, UMR5805 EPOC, University of Bordeaux, 33615 Pessac, France

9 *To whom correspondence should be addressed;

10 E-mail: alberto.baudena@gmail.com.

11 **Abstract**

12 Plastic is a widespread marine pollutant, with most studies focusing
13 on the distribution of floating plastic debris at the sea surface. Recent evi-
14 dence, however, indicates a significant presence of such low density plastic
15 in the water column and at the seafloor, but information on its origin and
16 dispersion is lacking. Here, we studied the pathways and fate of sinking
17 plastic debris in the Mediterranean Sea, one of the most polluted world
18 seas. We used a recent Lagrangian plastic-tracking model, forced with
19 realistic parameters, including a maximum estimated sinking speed of 7.8
20 m/d. Our simulations showed that the locations where particles left the
21 surface differed significantly from those where they reached the seafloor,
22 with lateral transport distances between 119–282 km. Furthermore, 60%
23 of particles deposited on the bottom coastal strip (20 km wide) were re-
24 leased from vessels, 20% from the facing country, and 20% from other
25 countries. Theoretical considerations furthermore suggested that biological
26 activities potentially responsible for the sinking of low density plastic
27 occur throughout the water column. Our findings indicate that the res-
28 sponsibility for seafloor plastic pollution is shared among Mediterranean
29 countries, with potential impact on pelagic and benthic biota.

30 **Keywords:** low-density plastic, marine pollution, water column, seafloor, trans-
31 port, sinking speed

32 **Synopsis:** Minimal information is available on the fate of plastics sinking from
33 sea surface. Here we show that they potentially travel hundreds of km and that
34 accountability for seafloor pollution is shared among Mediterranean countries.

35 **1 Introduction**

36 Plastic pollution represents a major threat to the oceans, causing socio-economic
37 damage and impacting tourism, fishing, and marine ecosystems (1, 2). More
38 than 914 marine species have been reported to accidentally ingest or be en-
39 tangled by plastic, a number expected to increase in the near future (3). In

40 addition, plastic debris is a vector for invasive species and persistent organic
41 pollutants (4, 5, 6). Around 300,000 metric tons of plastic have been estimated
42 to float at the sea surface (7). However, they only represent a tiny portion of the
43 plastic expected to enter the marine environment each year (8, 9, 10), suggest-
44 ing that plastic may be even more present in other ocean compartments. Even
45 if the amount of plastic entering the oceans (e.g., via rivers) and the plastic
46 budget are still open questions (10, 11, 12), a growing body of evidence suggests
47 that plastic debris is present not only at the sea surface, but in the whole water
48 column and sea bottom (e.g. refs. 13, 14, 15, 16, 17, 18). Surprisingly, observa-
49 tions reported plastic debris composed of polymers lighter than seawater in the
50 water column, down to at least 1000 m depth (14).

51 Several processes are responsible for the removal of plastic debris from the sea
52 surface, the most studied being biofouling (19, 20) - the colonisation of plastic
53 debris by bacteria, algae or invertebrates - which increases its relative density.
54 This process continues until, eventually, the debris leaves the surface, and has
55 been documented by laboratory and, recently, by in situ studies (21, 22, 23, 24).
56 Other processes that could lead to the removal of surface plastic debris are ag-
57 gregation in marine snow and faecal pellet formation after ingestion (25, 26).
58 However, information about the pathways and fate of settling plastic debris is
59 lacking. A common assumption is that plastic debris reaches the seafloor where
60 it has left the surface (27). This assumption has also been used to estimate the
61 seafloor plastic concentration (16).

62 The aim of this study is to assess the validity of this assumption and to im-
63 prove the understanding of plastic transport from the sea surface to the sea
64 bottom. This information is essential to solve the plastic budget problem, to
65 understand plastic fate, and for mitigation strategies. For that purpose, we use a
66 Lagrangian plastic-tracking model to analyse (i) the potential pathways of plas-
67 tic debris from the surface to the seafloor, (ii) its distribution once it reaches
68 the seafloor, and (iii) its potential sources. We focus on plastic whose absolute
69 density is lighter than seawater (referred to as low-density plastic, LDP), usually
70 smaller than 5 mm in size (28). This includes low- and high-density polyethy-
71 lene and polypropylene, which represent 88% of the LDP debris floating at the
72 surface of the Mediterranean Sea (29), and about half of the produced plastic
73 globally (30, 6). We only focus on the sinking phase of LDP debris, as multiple
74 works already studied its cycle from the moment it is released at sea until it
75 starts sinking (e.g. (31, 27, 32)). We do not consider high density plastic de-
76 bris, which is expected to sink directly to the seafloor (17, 33) and about which
77 there is little information, nor extremely light items which mainly float at the
78 air-sea interface. Lagrangian methods are widely used to describe the transport
79 of particles in the ocean and are suited to describe the transport of LDP debris.
80 These models can cover areas wider than observations and can describe forward
81 and backward trajectories useful to identify sources and pathways.

82 This study is a first modeling effort to evaluate the transport dynamics and fate
83 of LDP in the Mediterranean Sea, which is an ideal case study for two main
84 reasons: (i) globally, it is one of the most plastic polluted seas (28, 34); (ii)
85 its plastic pollution at the sea surface has been intensively studied, allowing us
86 to estimate key physical parameters such as plastic debris sinking speed and to
87 set initial conditions. In particular, we combine recent observations of plastic
88 concentration in the water column, the largest Mediterranean Sea database of
89 floating LDP debris to date, one of the best performing drag models, and esti-

90 mates of the location and amount of LDP leaving the sea surface. The latter
91 metric was obtained from the first Lagrangian model quantitatively validated in
92 the Mediterranean Sea (31), by assuming that the probability of a LDP leaving
93 the surface increases with the time it spent in water according to a prescribed
94 function. With this information, we are also able to calibrate the model and
95 perform a detailed sensitivity test. We then provide an assessment of the paths
96 and fate of LDP sinking in the Mediterranean sea as well as an estimation of
97 the contribution of the different countries to the coastal seafloor pollution. Fi-
98 nally, we consider the implications of the calculated density differences between
99 generic sinking LDP debris and seawater to assess the role of biological transport
100 throughout the water column, consistent with recent studies.

101 2 Materials and Methods

102 2.1 The numerical Lagrangian model: velocity field and 103 trajectory computation

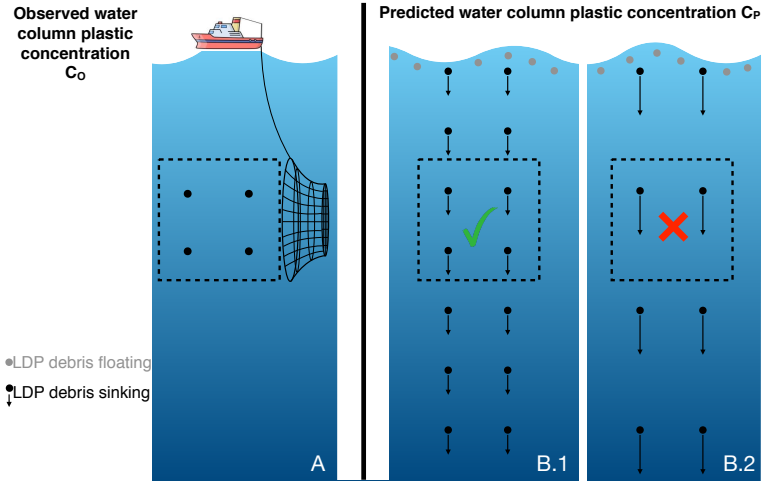
104 Here, we simulate the path of LDP debris once they start sinking from the sur-
105 face (due to biofouling or other processes) down to 1000 m. We do not analyse
106 what occurs to debris prior to that (i.e., from the moment it was released at
107 sea to when it left the sea surface), as several studies already investigated this
108 question (e.g. (31, 27, 35)). Hence, this study can be seen as a continuation
109 of those works. To this aim, we used the TrackMPD model (36), an advanced
110 3D Lagrangian model recently developed to simulate the fate of plastic debris
111 at sea. The TrackMPD model reads the velocity field offline, and computes the
112 trajectories with a Runge-Kutta scheme of order 4-5 both in time and space.
113 Time steps were set to 3 hours. Model initialisation and simulated scenarios are
114 reported in Subsec. 2.3.

115 The velocity field used to simulate the virtual particle trajectories was a high
116 resolution configuration of the NEMO model (NemoMed36; $1/36^\circ \times 1/36^\circ$) pro-
117 vided at daily intervals, with 50 stretched vertical levels (sigma coordinate sys-
118 tem), developed by Arsouze et al. (37). This circulation model was initialised
119 with sea surface temperature and salinity fields and took into account riverine
120 freshwater runoff. It included the vertical component of the velocity field w as
121 well. This product has already been used to simulate 3D virtual plastic trajec-
122 tories in the Mediterranean Sea (38).

123 A Stokes component was added to the NemoMed36 velocity field. The Stokes
124 product (MEDSEA_HINDCAST_WAV_006.012), with a spatial resolution of
125 $1/24^\circ$, was spatially interpolated over the grid of NemoMed36, and was summed
126 to its upper layer. This allowed us to take into account Stokes drift due to waves
127 at the surface, which affects particles in the first meters of their sinking. Stokes
128 effect indirectly includes windage and is known to affect plastic fate (39).

129 2.2 Constraining the model settings

130 A key parameter to study the fate of (biofouled) sinking LDP debris in the
131 water column is its settling speed. In situ observations of LDP settling speed
132 are not available to date. A few studies have measured the settling velocity of
133 biofouled plastic particles under laboratory conditions and found that a large
134



130

131 Figure 1: Illustrative scheme of the paradigm used to calculate the sinking speed
 132 of LDP debris. The predicted water column LDP concentration C_P decreases
 133 when LDP sinking speed increases (panels B.1 and B.2). In order to have C_P
 134 equal or greater to a given value observed C_O (panel A), the LDP sinking speed
 135 must not be larger than a given value. In this case panel B.1 represents the
 136 maximum possible sinking speed of LDP debris. Panel B.2 shows that, if a
 137 larger sinking speed is considered, then C_P is lower than C_O .

143 number of parameters, both physical (e.g. particle polymer, shape and size;
 144 water temperature and salinity) and biological (e.g. biofilm growth and den-
 145 sity) can impact the sinking speed (33, 24, 19). The large spectrum of sinking
 146 LDP and environmental conditions in the ocean make difficult the definition
 147 of settling speed in numerical simulations. For these reasons, we calculated a
 148 (maximum) representative sinking speed value to calibrate our model, ensuring
 149 that mean simulated and observed LDP concentrations in the water column
 150 have the same order of magnitude. We assumed that the water column LDP
 151 concentration is the result of a linear fall of LDP debris from the sea surface.
 152 The larger the LDP sinking speed, the lower the water column LDP concentra-
 153 tion for a given rate of plastic submergence from surface (Fig. 1). By taking the
 154 lowest water column LDP concentration measured to date as the lower bound-
 155 ary, we can derive a maximum sinking speed, which will be the reference value
 156 in the simulations. Details of the calculation are provided in the following sub-
 157 sections. The choice of a linear fall of LDP debris is evaluated by integrating
 158 the largest LDP database in the Mediterranean Sea to date ($\sim 75,000$ debris)
 159 and with a drag model (Subsec. 2.5).

160 2.2.1 Observed water column plastic concentrations C_O

161 Here, we report the current literature on observed plastic concentrations in the
 162 ocean water column (hereafter C_O) in Table 1 (adapted from Liu et al., (40))
 163 which is used to calibrate the simulated plastic concentration in the model. We
 164 did not consider the measurements sampled at a depth shallower than 50 m to
 165 exclude mixing layer processes, except for the study of Lattin et al., (41), as it is

166 among the only 4 studies which measured the LDP mass concentration ($\mu\text{g}/\text{m}^3$)
167 to date. The highest concentrations were measured by Pabortsava et al., (42)
168 ($940 \mu\text{g}/\text{m}^3$) and Lattin et al., (41) ($150 \mu\text{g}/\text{m}^3$), the lowest by Egger et al.,
169 (14) ($1.6 \mu\text{g}/\text{m}^3$, averaged on the 5–1000 m depth layer).
170 Four studies measured C_O in coastal areas of the Mediterranean Sea (43, 15,
171 44, 45). Baini et al., (43) and Lefebvre et al., (15) found similar concentrations
172 (0.23 ± 0.20 particles/ m^3 ; 0.26 ± 0.33 particles/ m^3 , respectively). Vasilopoulou et
173 al., (44) and Rios-Fuster et al., (45), sampling in shallower waters (< 50 m), and
174 close to the coast, found water column plastic concentration ~ 200 times larger
175 (41 ± 22 and 67 ± 52 particles/ m^3 , respectively). Interestingly, Rios-Fuster et al.,
176 (45) found LDP debris down to 50 m depth.
177 As the studies on the Mediterranean Sea did not measure the mass of plastic
178 debris, we compared them with the concentrations of Egger et al., (14) which
179 reported the lowest concentrations in $\mu\text{g}/\text{m}^3$ and particles/ m^3 and can serve as a
180 reference value of minimum plastic concentration in the water column to obtain
181 in our simulations. Egger et al., (14) collected LDP debris larger than $500 \mu\text{m}$,
182 76% of plastic debris collected by Baini et al., (43) was larger than $500 \mu\text{m}$, while
183 the mean size of plastic debris found by Lefebvre et al., (15) was (1.81 ± 1.42)
184 mm, indicating that most of debris was larger than $500 \mu\text{m}$. Therefore, Egger
185 et al., (14), Baini et al., (43), and Lefebvre et al., (15) studies collected plastic
186 debris of similar size range, but the concentration measured by Egger et al.,
187 (14) was ~ 200 times lower (0.001 particles/ m^3). Hence, Mediterranean water
188 column plastic concentrations are probably larger than those measured by Egger
189 et al., (14) also when considering the mass ($\mu\text{g}/\text{m}^3$). This is also corroborated
190 by the fact that the Mediterranean is one of the seas most affected by plastic
191 pollution, with surface LDP concentrations comparable to those found in the
192 North Pacific Garbage Patch (NPGP) (28, 34, 43). Biofouling was predicted to
193 be larger in several regions of the Mediterranean Sea than in the oligotrophic
194 NPGP area (32), suggesting that more LDP particles might leave the surface
195 in the Mediterranean. However Mediterranean Sea studies (43, 15, 44) sampled
196 lower water volumes, inducing possible biases towards higher concentrations (46,
197 40, 47). Therefore, we considered a minimum water column LDP concentration
198 $C_{O_{MIN}} = 1.60 \mu\text{g}/\text{m}^3$

Sampling regions	Methods	Samples pretreatment and polymer analysis	Volume/sample (L)	Depth (m)	Mesh size of nets ^a or filters (sieves) ^b (µm)	MP's size (mm)	Plastic concentration (items/m ³)	Plastic concentration (µg/m ³)
Arctic Central Basin (Kashai et al., 2018, ref. 48)	CTD sampler	Direct filtration; µ-FTIR spectrometer	7-48	8-1370	250 ^a ; 120 ^b	0.25-5.00	0-100	/
Mariana Trench (Peng et al., 2018, ref. 49)	CTD sampler	Direct filtration; Raman spectroscopy	35-180	2,673-10,904	0.22 ^b ; 0.30 ^b	1.00-3.00 (mostly) ^c	(2-14)·10 ⁶	/
Baltic Sea proper (Buguev et al., 2017, ref. 50)	CTD sampler	Direct filtration; Combination of visual identification and UV lamp	7.79-30	0.5-217.5	174 ^b	N/A ^d	80 (fibers)	/
Sumba coastal waters, Indonesia (Cordova et al., 2018, ref. 51)	CTD sampler	Direct filtration; FT-IR spectrometer	10	5-300	0.45 ^b	0.30-1.00 (mostly) ^c	44±25	/
Baltic Sea, Sweden (Gorokhova, 2015, ref. 52)	Plankton net	Direct observation; visual identification	6,200-9,200	0-100	90 ^a	0.05-0.30 (mostly) ^c	2000-3000	/
Tusany coastal waters, Mediterranean Sea (Zhu et al., 2018, ref. 43)	Plankton net	Direct observation; FT-IR spectrometer	500-30,000	2-120	200 ^a	1-2.5 (mostly) ^c	0.26	/
Gulf of Lions (Leclercq et al., 2019, ref. 15)	Plankton net	Direct observation; FT-IR spectrometer	N/A ^d	0-100	200 ^a	0.24-4.93	0.23±0.20	/
Cyprus coasts (Vassilopoulou et al., 2021, ref. 44)	Plankton net	Direct observation; DMIL microscope and SLX-3 stereoscope	N/A ^d	0-50	200 ^a	0.2-5	41.31±22.41	/
Spanish coast (Rios-Fuster et al., 2022, ref. 45)	Niskin bottles	Direct filtration; FT-IR spectrometer on 10% of items	5	5-50	1.2 ^b	0.1-8.4	1860±1430 (67 without fibers)	/
Northeast Pacific (Goldstein et al., 2013, ref. 53)	Plankton net	Direct observation; FT-IR spectrometer	N/A ^d	0-210	202 ^a	N/A ^d	0.05	/
Santa Monica Bay (Lain et al., 2004, ref. 41)	Multi-net trawls	Freshwater floatation; No polymeric identification	N/A ^d	0-14.80	333 ^a	2.80-4.75 (mostly) ^c	/	150
North Pacific Garbage Patch (Egger et al., 2020, ref. 14)	Multiple Opening and Closing Net	Direct observation; Raman spectroscopy	136,000-5,039,000	0-2,003	333 ^a ; 500-15,000 ^b	N/A ^d	0.001	1.60
Baltic Sea, Russia (Zubkov et al., 2019, ref. 54)	Submersible pump	Organics removal prior to the refiltration (174µm); µ-Raman spectroscopy	2,500-3,500	0.5-91	174 ^b	0.17-1.00 (mostly) ^c	32	/
Korean coastal waters (Song et al., 2018, ref. 55)	Submersible pump	NaCl solution floatation prior to the refiltration; µ-FT-IR spectrometer	100	3-58	20 ^b ; 5 ^b	0.02-5.00	423 (50 if only particles < 5 mm)	/
Monterey Bay (Chow et al., 2019, ref. 13)	In-situ filtration device	Direct observation; Raman spectroscopy	1,007-2,378	5-1,001	100 ^b	N/A ^d	1-10	/
HAUSGARTEN observatory (Eckman et al., 2020, ref. 56)	In-situ filtration device	Organics removal prior to the filtration; µ-FT-IR spectrometer	218-561	1-5,351	32 ^b	0.01-0.15	95±85	/
West Pacific and East Indian Ocean (Li et al., 2020, ref. 47)	In-situ filtration device	Wet peroxide oxidation; µ-FT-IR spectrometer	10,000	2-4001	60 ^b ; 1.60 ^b	0.03-6.33 (mean 0.07)	0.2-3.5	/
Atlantic Ocean (Fabrisova et al., 2020, ref. 42)	In-situ filtration device	Organics removal prior to the filtration; µ-FT-IR spectrometer	500-1500	0-201	55; 25	0.032-0.651	2300	940
Atlantic Ocean (Zhao et al., 2022, ref. 57)	Multiple Opening and Closing Net; WTS-LV pump	Direct observation; visual identification; µ-FT-IR spectrometer	440-1765	0-5200	200 ^a	SMP: <100µm; LMP: >300µm	SMP: 0.244.3; LMP: 0.0011	SMP: 0.20.83; LMP: 0.15.3

a: mesh size of net used in the reference.
b: mesh size of filter or sieve used in filtering process.
c: only size range of MPs was presented in the literature.
d: N/A represented no available information.

Table 1: Literature on Mediterranean water column plastic concentration (adapted with permission from Liu et al., (40), Copyright 2020 Elsevier).

203 **2.2.2 Annual estimates of LDP plastic entering the Mediterranean**
 204 **Sea.**

205 We defined N_{TBY} as the number of tons of LDP leaving the Mediterranean
 206 surface every year due to biofouling or other processes. N_{TBY} was obtained
 207 assuming that $\sim 11.5\%$ of the amount of floating plastic debris entering the
 208 Mediterranean Sea every year from coastal sources or vessel discards (N_{LDPY})
 209 left the sea surface during that period due to biofouling or other processes. This
 210 percentage was based on the study by Baudena et al., (31), and was similar to
 211 the value obtained in a previous study (9.2 %, 27). Thus:

$$N_{TBY} = 0.115 \cdot N_{LDPY} . \quad (1)$$

212 N_{LDPY} was estimated using the findings of ref. (8). The authors calculated the
 213 number of tons of plastic debris entering the global ocean in 2010. Considering
 214 that $\sim 50\%$ of plastic is LDP (mainly low- and high-density polyethylene and
 215 polypropylene, 30, 6), about 100,000 tons of LDP debris were estimated to enter
 216 the Mediterranean Sea in 2010. This quantity includes also extremely light and
 217 large LDP not considered here. However, these constitute less than 1% of items
 218 collected in the Mediterranean Sea (28). Overall, the assumed quantity repre-
 219 sents a compromise between recent estimates, both lower (58, 59) and higher
 220 (11, 10). Furthermore, we stress that this value was adopted in recent studies
 221 modelling plastic-debris dispersion in this basin (27, 38, 31). The sensitivity
 222 of the results with respect to this parameter is studied by simulating a further
 223 scenario (Subsec. 2.3).
 224

225 **2.2.3 Estimation of the maximum sinking speed of LDP debris SS_{MAX}**

226 N_{TBY} can be converted into a flux F of LDP mass leaving each m^2 of sea surface
 227 every day by considering the Mediterranean surface ($\simeq 2.5 \times 10^{12} m^2$):

$$F = \frac{N_{TBY} \cdot 10^6}{365 \cdot 2.5 \cdot 10^{12}} \frac{g}{dm^2} = 1.10 \cdot 10^{-9} N_{TBY} \frac{g}{dm^2} \quad (2)$$

228 The predicted concentration of the falling particles in the water column C_P
 229 (expressed as g/m^3) depends on their vertical sinking velocity SS . We stress
 230 that the flux of particles sinking from the sea surface is a release of individual
 231 particles (the LDP debris) at discrete intervals (Fig. 1), similar to a *rain effect*.
 232 Thus, the concentration C_P was considered as the ratio between F (Expr. 2)
 233 and SS (expressed in m/d, Fig. 1):

$$C_P = \frac{F}{SS} = \frac{N_{TBY}}{SS} 1.10 \cdot 10^{-9} \frac{g}{m^3} \quad (3)$$

234 Expr. (3) implies that the more slowly LDP debris sinks, the greater the re-
 235 sulting water column plastic concentration is, and vice versa (Fig. 1, panels B.1
 236 and B.2). If N_{TBY} increases (and we assume the same sinking speed), so does
 237 the water column plastic concentration. Here, C_P was derived considering the

238 same sinking speed and mass for all the particles. We also derived an expres-
 239 sion for the predicted concentration by considering individual sinking speed and
 240 mass, and showed that these did not affect C_P , nor the conclusions of our paper
 241 (Supporting Information S.1).

242 By inverting Expr. (3), we could obtain an expression for the sinking speed of
 243 the LDP debris, SS :

$$SS = \frac{N_{TBY}}{C_P} 1.10 \cdot 10^{-9}, \quad (4)$$

244 from which it was possible to obtain a maximum estimate of the settling speed
 245 SS_{MAX} in the Mediterranean Sea. To do so, we considered the estimate of
 246 N_{TBY} for the Mediterranean Sea (11,500 tons/year, Subsec. 2.2.2) and imposed
 247 $C_P=C_{O_{MIN}}$ ($1.60 \mu\text{g}/\text{m}^3$, Egger et al., (14), Subsec. 2.2.1):

$$SS_{MAX} = \frac{N_{TBY}}{C_{O_{MIN}}} 1.10 \cdot 10^{-9}, \quad (5)$$

248 By substituting these values in Expr. (5), we obtained $SS_{MAX}=7.8$ m/d.

249 In summary, in order to have a minimum water column plastic concentration
 250 of $1.60 \mu\text{g}/\text{m}^3$, considering a maximum load of 11,500 tons of biofouled LDP
 251 leaving the surface each year, LDP debris should sink with a maximum settling
 252 speed of 7.8 m/d. Considering a greater water column plastic concentration,
 253 and/or a lower load of biofouled LDP per year would lead to a lower sinking
 254 speed.

255 We stress that using the C_O values of Baini et al., Lefebvre et al., Vasilopoulou et
 256 al., (43, 15, 44) (converted in plastic mass) as $C_{O_{MIN}}$ rather than those of Egger
 257 et al., (14), SS_{MAX} would have been lower. Similarly, using a lower N_{LDP_Y} (and
 258 thus a lower N_{TBY}) would have lead to a lower SS_{MAX} value. Nevertheless,
 259 we considered a two fold value of N_{TBY} , by carrying out a simulation with a
 260 sinking speed set to twice SS_{MAX} (15.6 m/d, Subsec. 2.3).

261 **2.3 Model initialisation and simulated scenarios**

265 The simulated particles were considered representative of LDP debris of all sizes,
 266 with the exception of extremely light foamed plastics (such as polystyrene foam)
 267 or air filled objects which tend to stay suspended at the air-sea interface. The
 268 latter represent less than 1% of plastic debris collected in the Mediterranean
 269 Sea (28). In general, 95% of LDP debris collected in the Mediterranean Sea
 270 are less than 5 mm in size (28). LDP debris were considered to sink, assuming
 271 that biofouling, weathering or other processes decrease the buoyancy of these
 272 particles. Virtual LDP particles were released at the surface at daily intervals
 273 between January 1, and December 31, 2010. This time interval is consistent
 274 with the residence time of plastic debris at the Mediterranean surface (31, 27).
 275 To initialise the particle starting positions, we used the results of Baudena et
 276 al., (31), which simulated the path of LDP debris from their release at sea (by
 277 coastal cities, river mouths, and vessels) to the moment they started sinking.
 278 In that work, the authors assumed that the probability of a simulated LDP
 279 particle leaving the sea surface (due to e.g. biofouling, etc.) increases with
 280 the time spent in water. This probability peaked in correspondence with the

281 biofouling time (the period of time necessary to induce sinking, see Supplemen-
282 tary Fig. 2 in Baudena et al., 31). In this way, the authors calculated the
283 Mediterranean surface sinking rate (the amount of LDP debris that disappears
284 from the surface each day in a square kilometer of sea surface). To strengthen
285 that metric Baudena et al., (31) considered different biofouling times (between
286 50–200 days, based on literature values) and obtained similar estimates when
287 considering 16 different parameterisations and an ensemble average. Hence, in
288 our study, particles were released proportionally to the Mediterranean surface
289 sinking rate, i.e. the larger the surface sinking rate in a region, the larger the
290 number of particles released there. The choice of the dataset of Baudena et
291 al.(31) is further motivated by the fact that it was the first Lagrangian model
292 quantitatively validated in the Mediterranean Sea.

293 7,652,197 virtual particles were released in total, using four sinking speed values
294 (7.8 m/d, Scenario 1; 4 m/d, Scenario 2; 2 m/d, Scenario 3; 1 m/d, Scenario
295 4; Table 2). The choice of the maximum value used for the sinking speed
296 ($SS_{MAX}=7.8$ m/d) is motivated in Subsec. 2.2. All virtual plastic particles
297 of a given scenario were advected for a time period (provided in Table 2) long
298 enough to reach at least 1000 m depth. For scenario 4 (sinking speed of 1 m/d),
299 particles were advected for 1000 days. At the end of the simulation, 90% of
300 particles reached 1000 m depth or were deposited. The 10 % left were at an
301 average depth of 900 ± 100 m, thus very close to reaching 1000 m depth. Thus,
302 we use their final position to calculate the seafloor concentration (Subsec. 2.4).
303 The particles were considered as non-inertial passive tracers with a constant
304 sinking velocity, which were transported by currents and by isotropic horizontal
305 and vertical diffusion (diffusivity coefficient K_h and K_v , respectively).

306 We used $K_h=10$ m²/s and $K_v=5\cdot 10^{-5}$ m²/s, in line with the values used in pre-
307 vious plastic studies (27, 36, 58, 31). In order to test the sensitivity of the results
308 to the choice of the diffusivity coefficients, different K_h and K_v values were used
309 (Scenarios 5–8, Table 2). In order to evaluate the role of the vertical component
310 of the current field w on the simulated LDP concentration, w was set to zero
311 in scenario 9 (Table 2). Scenarios 5–9 were run with the same sinking speed of
312 Scenario 1, namely 7.8 m/d. In order to evaluate the sensitivity of the results
313 with respect to a potentially larger SS_{MAX} (which could be due to a larger flux
314 of LDP leaving the surface, Subsec. 2.2.3), in Scenario 10 we used a sinking
315 speed of 15.6 m/d. Finally, in Scenario 11 we evaluated the sensitivity of the
316 results with respect to the release conditions: to do so, the surface sinking rate
317 of Baudena et al. (31) was varied at each location of $\pm 10\%$ randomly. This new
318 sinking rate was used to initialise the particle release locations of that scenario.

319

320 2.4 Model output analyses

321 One of the limitations in simulating particle trajectories from the surface to the
322 seafloor in a deep basin such as the Mediterranean Sea is the elevated compu-
323 tational cost. To overcome this issue, we calculated the concentration of the
324 simulated particles on a virtual layer at 1000 m depth. In the regions with a
325 seafloor shallower than 1000 m, we kept the original depth (provided by the ve-
326 locity field domain (37)). 1000 m was chosen as the reference depth because it is
327 usually considered as the upper boundary of the deep sea. Thus, LDP reaching
328 this layer are therefore considered as sequestered in the deep sea. Furthermore,

N° Scenario	Current velocity field	Vertical component of currents included (yes/no)	Sinking speed particles (m/d)	Release period	Advective period (days)	K_h (m ² /s)	K_v (m ² /s)	Notes
S1	NemoMed36	yes	7,8	1 Jan-31 Dec 2010	450	10	$5 \cdot 10^{-5}$	
S2	NemoMed36	yes	4,0		550			
S3	NemoMed36	yes	2,0		1050			
S4	NemoMed36	yes	1,0		1050			
S5	NemoMed36	yes	7,8		450	5	$5 \cdot 10^{-5}$	
S6	NemoMed36	yes	7,8		450	15		
S7	NemoMed36	yes	7,8		450	10	$1 \cdot 10^{-5}$	
S8	NemoMed36	yes	7,8		450		$10 \cdot 10^{-5}$	
S9	NemoMed36	no	7,8		450	10	$5 \cdot 10^{-5}$	
S10	NemoMed36	yes	15,6		225	10	$5 \cdot 10^{-5}$	
S11	NemoMed36	yes	7,8		450	10	$5 \cdot 10^{-5}$	Surface sinking rate varied of $\pm 10\%$

262

264

Table 2: Parameters used for each of the ten simulated scenarios.

329 this assumption allowed us to simulate sinking speeds down to 1.0 m/d, which
330 would not have been possible for further depths due to computational costs.
331 The concentration on a deeper virtual seafloor, at 2000 m depth, was calculated
332 for scenarios 1–3 only, and is reported in Supporting Information S.2.

333 Further, we calculated the concentration of particles deposited less than 20 km
334 from the coast (hereafter the coastal strip). We chose this distance because it is
335 associated with the inner average continental shelf, exploited by industrial and
336 recreational fishery and essential for tourism activity (60, 61). This concentra-
337 tion was calculated for each Mediterranean country. For each deposited particle
338 we identified if it was released by a land (coastal city or river mouth) or a sea
339 (vessel discard) source. To this aim, we tracked each particle backward in time
340 from the seafloor to the surface (using our trajectories) and from the surface to
341 its release source (using the trajectories calculated by Baudena et al., 31). If the
342 original release source was land based, we determined the corresponding source
343 country as well. The plastic sources considered were those used in Baudena et
344 al., (31), coastal cities (62), river mouths (63), and vessel discards (64).

345 We analysed the connectivity between Mediterranean surface and seafloor by
346 considering the starting and final position of each particle and by calculating
347 a connectivity matrix (65) at two different resolutions. Further details are re-
348 ported in Supporting Information S.3.

349 To understand the pathways of the LDP particles reaching a zone of high LDP
350 concentration, located north-east of the Balearic archipelago (Fig. 3A), we cal-
351 culated their crossroadness (66, 31). This metric provides, for a given point, the
352 percent of the trajectories that passed in its neighborhood (defined as a circle
353 of radius 0.1°). Further details are reported in Supporting Information S.4.

354 2.5 Density of sinking LDP debris from a drag model

355 In Subsec. 2.2.3, we estimated a maximum sinking speed SS_{MAX} of LDP debris
356 equal to 7.8 m/d. Here we calculate the difference of LDP and seawater densities

357 necessary to obtain such value. To this aim we use (i) the largest LDP debris
 358 dataset collected in the Mediterranean Sea to date and (ii) the drag model of
 359 Dioguardi et al., (67).

360
 361 **Mediterranean Sea LDP debris database**

362 We exploited the largest LDP field dataset in the Mediterranean Sea to date,
 363 collected during the Tara Expedition (122 stations, ref. 28,
 364 <https://zenodo.org/record/5538238>). This dataset provided the ferret (considered
 365 representative of the particle size d_p), sphericity Φ , and circularity χ of
 366 each LDP debris collected at the sea surface (75,030 items in total). We used
 367 these debris physical properties to estimate the velocity at which they are expected
 368 to sink once biofouled.

369
 370 **Drag model to calculate the sinking velocity**

371 Van Melkebeke et al., (68) evaluated eleven drag models estimating the vertical
 372 sinking velocities of plastic particles with different characteristics, such as size,
 373 shape, and density. The best performing drag model was the one reported in
 374 (67, average error of 13.20%), which calculated the vertical sinking speed SS_{DM}
 375 as follows:

$$SS_{DM} = \sqrt{\frac{4gd_p\Delta\rho}{3C_d\rho_{SW}}}, \quad (6)$$

376 where g is the gravity acceleration (9.81 m/s²), d_p is the particle size, $\Delta\rho$ is the
 377 difference between the particle density and that of seawater, ρ_{SW} . C_d is the
 378 particle drag coefficient, which the authors expressed as follows:

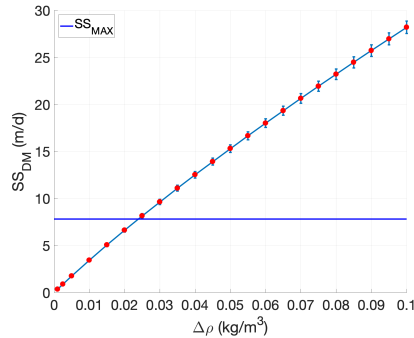
$$C_d = \frac{24}{Re_p} \left(\frac{1 - \Psi}{Re_p} + 1 \right)^{0.25} + \frac{24}{Re_p} (0.181 Re_p^{0.65}) \Psi^{-Re_p^{0.08}} + \frac{0.4251}{1 + \frac{6881}{Re_p} \Psi^{5.05}},$$

379 where Re_p is the particle Reynolds number.

$$Re_p = \frac{\rho_{SW} SS_{DM} d_p}{\mu_f},$$

380 with μ_f being the water dynamic viscosity. The range of validity of Eq. (6)
 381 is $0.03 < Re_p < 10^4$, which was respected with the parameters used. Ψ is the
 382 shape factor, defined as the ratio between the particle sphericity Φ and circularity χ .
 383 The vertical sinking velocity SS_{DM} depends therefore on the six
 384 parameters, d_p , $\Delta\rho$, ρ_{SW} , μ_f , Φ , and χ . We considered a seawater density
 385 $\rho_{SW}=1027$ kg/m³ and a viscosity $\mu_f=0.00109$ Pa·s; the latter is representative
 386 of a seawater temperature of 20° (https://www.engineeringtoolbox.com/seawater-properties-d_840.html), which is the mean Mediterranean surface temperature.
 387 As d_p , Φ , and χ we used the d_p , Φ , and χ of each of the 75,030 debris
 388 collected during the Tara expedition (Subsec. 2.5). Therefore, $\Delta\rho$ represents
 389 the only unknown parameter in Expr. 6.

390
 391
 392 Different $\Delta\rho$ values were tested in Expr. (6), ranging from 0.001 to 0.1
 393 kg/m³. The Matlab function provided in Dioguardi et al., (67) was used to
 400



392

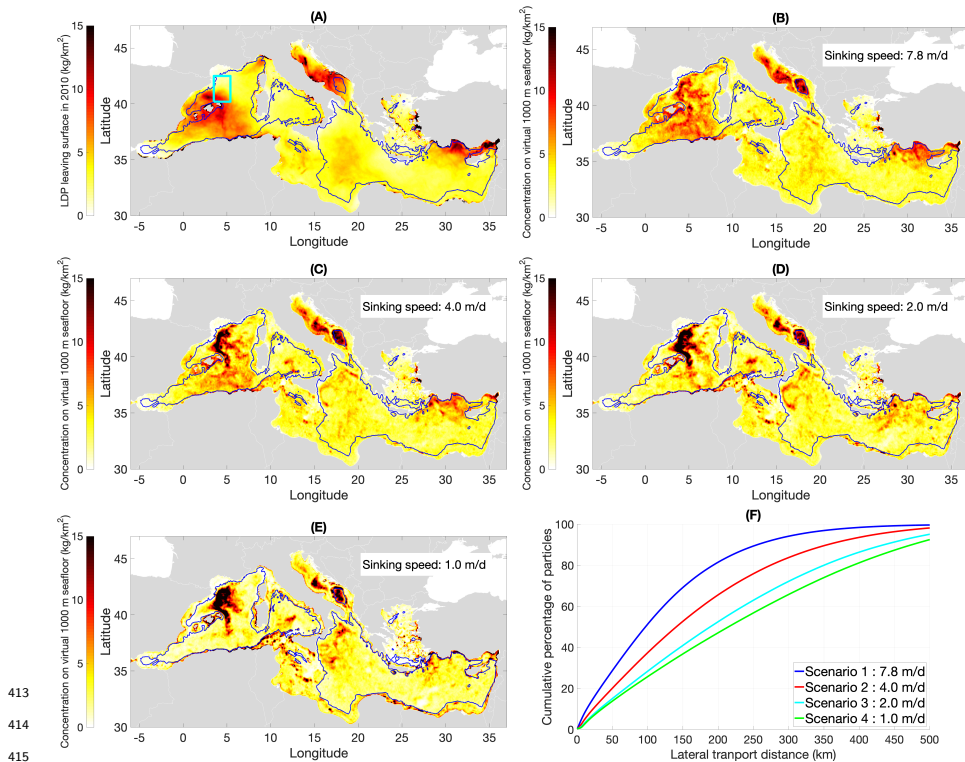
393 Figure 2: Mean theoretical sinking speed SS_{DM} of 75,030 LDP debris (y -axis,
 394 subsec. 2.5) as a function of the difference between the density of the biofouled
 395 LDP debris and the seawater $\Delta\rho$ (x -axis). SS_{DM} are reported as mean values
 396 (red dots) with standard deviation (errorbar). The blue horizontal line identifies
 398 the SS_{MAX} value calculated in Subsec. 2.2.3 (7.8 m/d).

401 calculate 75,030 SS values, which were then averaged together. We found that
 402 SS_{DM} matched SS_{MAX} for $\Delta\rho \simeq 0.025 \text{ kg/m}^3$ (Fig. 2). The $\Delta\rho$ obtained did
 403 not change considerably when the predicted water column plastic concentration
 404 C_P was calculated considering also the individual mass of each of the 75,030
 405 LDP debris (Supporting Information S.1). We also performed a sensitivity test
 406 to analyse the robustness of the mean SS_{DM} while varying the three other
 407 parameters d_p , ρ_{SW} , and μ_f . These calculations indicated that they did not
 408 affect the mean SS_{DM} value (Supporting Information S.5) significantly.
 409 Overall, above considerations show that only a minor excess density of 0.025
 410 kg/m^3 compared to seawater is required to reach a maximum sinking speed of
 411 7.8 m/d. Smaller $\Delta\rho$ are related to lower sinking speeds.

412 3 Results

430 3.1 Concentration of deposited LDP debris and distance 431 travelled during its sinking

441 The spatial distribution of particles deposited on the 1000 m depth virtual layer
 442 (Fig. 3B, C, D, and E;) was consistently different from the distribution of
 443 particles leaving the surface (Fig. 3A) for all the sinking speeds considered.
 444 When reducing the sinking speed, the difference increased (Fig. 3B to Fig. 3E).
 445 This result was particularly visible in the western Mediterranean: while large
 446 amounts of virtual particles were predicted to leave the surface north of the
 447 Balearic archipelago, the concentration at 1000 m depth in this same region
 448 was relatively low for all the scenarios considered. Conversely, the 1000 m con-
 449 centration was greater north-east of the Balearic archipelago, in a region where
 450 the surface sinking rate was lower (cyan rectangle in Fig. 3A). This region,
 451 covering 1.63% of the Mediterranean surface, contained 1.36% of the virtual
 452 LDP particles leaving the Mediterranean surface. Notably, at 1000 m depth, it
 453 accumulated the 3.07 %, 4.68%, 6.66%, and 7.36% of the virtual LDP particles
 454 for scenarios 1–4, respectively. The LDP particles deposited there were mostly



416 Figure 3: **(A)**: amount of virtual LDP particles that left the Mediterranean
 417 surface in 2010 (the surface sinking rate integrated between January 1, and
 418 December 31, 2010; kg/km²; adapted with permission from Baudena et al.,
 419 (31), Copyright 2022 Nature). **(B–E)**: concentration of virtual LDP particles
 420 released in 2010 deposited on a virtual seafloor at 1000 m depth, for scenario 1,
 421 2, 3, and 4, respectively. The virtual 1000 m seafloor was built by considering
 422 all the seafloor locations deeper than 1000 m as 1000 m deep. The blue lines
 423 in panel A–E indicate the 1000 m isobath. **(F)**: cumulative pdf of the lateral
 424 transport distance (the distance between the location in which the particle left
 425 the surface and the location in which it reached the virtual 1000 m seafloor) of
 426 the 7,652,197 virtual particles released in 2010, for scenario 1 (blue line), 2 (red
 427 line), 3 (cyan line), and 4 (green line). The cyan rectangle in panel (A) shows
 428 the region considered for the statistical analyses.

455 from the south and the east of this region, as supported by supplementary anal-
 456 yses (Supporting Information S.4)

457 The connectivity analysis between the locations where particles left the surface
 458 and where they reached the seafloor indicated that between 90–95% of the parti-
 459 cles (scenarios 1–4) deposited at a certain location (defined by a ~ 111 km size
 460 square) started to sink in other regions (Supporting Information S.3). In the
 461 Southern Adriatic Sea, where a hotspot of enhanced LDP accumulation was
 462 identified, between 32–50% of the particles were from adjacent regions. Other
 463 LDP accumulation regions were detected across the basin, such as in the Tyrre-
 464 nian and Ionian Seas, in the Strait of Sicily, or in the Eastern Mediterranean.

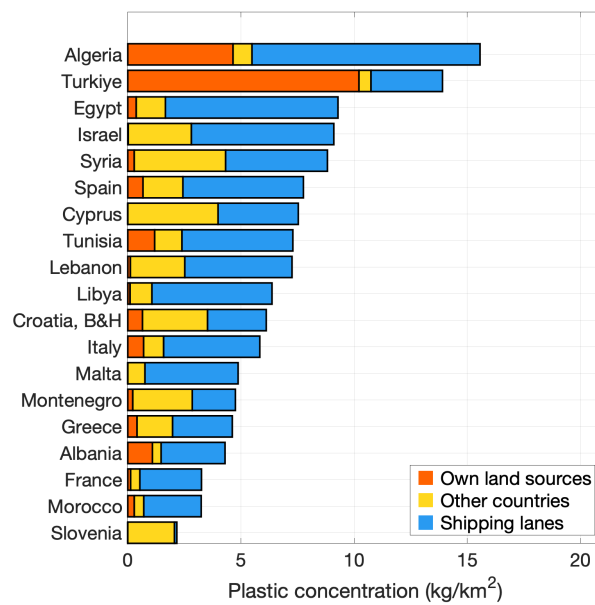
465 The spatial variability between the concentration of virtual LDP particles leav-
466 ing the surface and reaching the 1000 m virtual seafloor was confirmed also by
467 the cumulative pdf of the lateral transport distance (Fig. 3F). This was de-
468 fined as the distance between the locations at which particles left the surface
469 and those where they reached 1000 m depth. The mean lateral transport dis-
470 tance for scenario 1 was 119 ± 99 km; for scenario 2: 172 ± 136 km; for scenario
471 3: 232 ± 177 km; and for scenario 4: 282 ± 218 km. The percentage of virtual
472 LDP particles with a lateral transport distance larger than 100 km was 30%
473 for scenario 1, increasing to more than 60% for scenario 4. This conclusion was
474 robust to changes in the horizontal and vertical diffusivity, to the exclusion of
475 the vertical component of the velocity field, to the increase of the sinking speed
476 of the LDP particles up to the double of SS_{MAX} , and to changes of the surface
477 sinking rate used to initialise the particle starting locations (Supporting Infor-
478 mation S.6).

479 In situ observations of seafloor plastic concentration in the Mediterranean are
480 sparse in space and time and differ in methodology. In addition, these collected
481 all types of plastic, while here we focus on LDP only. Hence, a quantitative
482 comparison with our model results is currently not possible. Despite these con-
483 straints, our model predictions qualitatively agree with in situ measurements
484 (databases and their references in Supporting Information S.7). Largest seafloor
485 concentrations are reported in the Central Adriatic Sea, close to the Turkiye
486 shore, and in the Balearic archipelago, where our model predicts the largest
487 LDP concentrations. Conversely, the lowest concentrations were measured on
488 the Eastern Sardinia shelf, in the Northern Tyrrhenian Sea, and close to Alicante
489 (Spain), in agreement with our model predictions (further details in Supporting
490 Information S.7).

491 **3.2 LDP concentration on the coastal strip of Mediter-** 492 **anean countries**

493 The concentration of particles deposited on the coastal strip (i.e. in this study
494 within 20 km from the coast, Subsec. 2.4) ranged between 5.5–8.9 kg/km²
495 (scenarios 1–4), which was between 11–69% larger than the concentration of
496 particles sinking from the sea surface above (i.e., less than 20 km from the
497 coast; 5.2 kg/km²). The bottom coastal strips of Algeria and Turkiye showed
498 the largest particle concentrations (15.6 and 13.9 kg/km², respectively, obtained
499 from an ensemble average of scenarios 1–4; Fig. 4).

500 We tracked the particles deposited on the bottom coastal strip backward in time
501 (based on Baudena et al., (31), Methods), and we found that $\sim 60\%$ were from
502 vessel discards, while $\sim 40\%$ were released from land sources. On average, $\sim 20\%$
503 of the particles deposited on the coastal strip of a given country were from the
504 land sources of the same country, while $\sim 20\%$ were from other countries, with
505 some variability. For example, 53% of particles deposited on the coastal strip of
506 Cyprus were from neighbouring countries. The corresponding values for Croatia
507 and Syria were 47 and 46%, respectively. Conversely, 73% of particles deposited
508 on the coastal strip of Turkiye were from Turkish coastal sources. Finally,
509 83% of the particles deposited on the coastal strip of Egypt were from vessel
510 discards. This proportion was similar for particles deposited on the coastal strip
511 of Malta and Libya (84 and 83%, respectively). Results obtained for scenarios
512 1–4 separately (Supporting Information S.8) were consistent with this pattern.



432

433 Figure 4: Concentration of particles released in 2010 which deposited on the
 434 coastal strip (defined as the region less than 20 km from the coast) of the differ-
 435 ent Mediterranean countries, obtained from the ensemble average of scenarios
 436 1–4. For each country, the red rectangle represents the amount of particles de-
 437 posited on its coastal strip which were released from its own land sources, the
 438 yellow rectangle represents those released from other countries, and the blue
 439 rectangle those directly released at sea.

513 4 Discussion

514 4.1 Pathways and fate of sinking LDP debris

515 The study of the pathways of sinking LDP debris has highlighted that the loca-
516 tions where LDP debris left the surface did not coincide with the locations where
517 it was found at depth, as assumed by recent studies (27, 16). This stressed the
518 importance of a three dimensional approach to study plastic dispersion (69).
519 When neglecting the vertical component of the currents, the accumulation of
520 virtual LDP particles in specific regions slightly decreased, e.g. for the area
521 north-east of the Balearic archipelago (last panel in Fig. S.6). When con-
522 sidering a virtual seafloor down to 2000 m (Supporting Information S.2), the
523 accumulation slightly decreased as well. This indicated an important role played
524 by vertical current shear and by horizontal stirring on the accumulation of LDP
525 particles, in coherence with recent studies (70, 38). For instance, we observed
526 a region of LDP particle accumulation at 1000 m depth in the Adriatic Sea.
527 This matched remarkably well with a recently discovered persistent bottleneck
528 structure in the circulation of this sea (71), which may be responsible for this
529 LDP accumulation. In a specific region north-east of the Balearic archipelago,
530 the number of LDP debris deposited increased for slower sinking speeds. Cross-
531 roadness analyses indicated a possible mechanism of particle accumulation at
532 depth (Supporting Information S.4): particles are transported toward this area
533 due to the regional converging circulation. At the same time, particles sinking
534 more slowly spend more time suspended in the water column, traveling larger
535 distances. Hence, the probability they end up in that region increases.
536 Our simulations also pointed to the fact that a large fraction of LDP particles
537 could potentially reach the deep sea: 48–63 % of the virtual LDP particles leav-
538 ing the surface were transported to 1000 m depth, while 38–46 % reached 2000
539 m in Scenarios 1–3.

540 Even if further information is needed to quantitatively validate our model out-
541 puts, our results were in general agreement with in situ observations of seafloor
542 plastic concentration (Supporting Information S.7), corroborating our findings.
543 In addition, our results were robust with respect to horizontal and vertical dif-
544 fusivity changes, removal of the vertical velocity current component, variation
545 of the LDP debris sinking speed, and changes of starting sinking locations (Sup-
546 porting Information S.6).

547 4.2 Bottom coastal LDP pollution.

548 The estimated LDP concentration on the bottom coastal strip increased for
549 decreasing sinking speeds (from 5.6 kg/km² for 7.8 m/d sinking speed to 8.9
550 kg/km² for 1 m/d). This concentration was 11–69% higher than the concentra-
551 tion of LDP particles leaving the sea surface in the same region (5.2 kg/km²).
552 This indicated that currents at depth tend to propel debris towards coastal re-
553 gions. This agrees with the pattern of surface currents, which are expected to
554 retain LDP debris in the majority of Mediterranean coastal regions (27, 31).
555 Notably, ~ 20% of the particles deposited in the coastal region of a given coun-
556 try were from neighbouring countries, while ~ 60% were from maritime sources.
557 The high percentage of deposited LDP debris originating from maritime sources
558 (60%) is due to the fact that these particles spend more time at the surface

559 than particles released from land sources, which tend to strand quickly and are
 560 therefore less biofouled. In general, while previous studies suggested that each
 561 country is the primary responsible for the plastic pollution of its own beaches
 562 (27, 31), LDP debris on the bottom coastal strip seems to be from multiple
 563 Mediterranean countries and especially from shipping lanes. For instance, Egypt
 564 has been reported to have large rates of beaching plastic debris, mostly released
 565 from its own land sources (27, 31): however, we suggest that its coastal strip
 566 pollution is mainly due to LDP particles released at sea or from other countries.
 567 Overall, LDP pollution emerges as a shared problem in the Mediterranean basin,
 568 as particles polluting the bottom coastal strip were mostly released at sea or
 569 from distant countries.

570 **4.3 Implications from comparing the maximum sinking** 571 **speed SS_{MAX} with the sinking speed from a drag model** 572 **SS_{DM}**

573 Several biological processes are suspected to affect LDP debris throughout the
 574 water column. Kooi et al., (20) theorised a progressive colonisation of LDP,
 575 which is expected to decrease and eventually cease below the euphotic layer
 576 (due to mineralization or scraping of plastics by copepods; 72). Also, frag-
 577 mentation fosters the slowdown of settling LDP debris, as the vertical sinking
 578 velocity decreases with decreasing debris size (73). Hence, LDP debris may be
 579 resuspended and colonised again (20), as modelled by Lobelle et al., (32), Fischer
 580 et al., (70), and Tsiaras et al., (74). Other biological activities can occur below
 581 the euphotic zone, such as the biofilm formation via heterotrophic organisms
 582 that do not necessarily require light to grow (70). Aggregation in marine snow
 583 and consumption by zooplankton may cause plastic debris to sink, whereas rem-
 584 ineralization at depth would remove organic mass from plastic debris, making it
 585 rise again (75, 76). Zooplankton faecal pellets usually do not reach the seafloor
 586 due to coprophagy (see a review in 77), potentially releasing buoyant plastic
 587 debris. In addition, faecal pellets containing plastic debris are more subject
 588 to fragmentation (25), potentially enhancing resuspension. Chemical processes
 589 can affect the buoyancy of LDP debris as well, especially in regions where bio-
 590 logical activities are limited, such as in the NPGP. For example, weathering of
 591 debris causes hydrogen abstraction with oxygen substitution penetrating deeper
 592 into the polymeric matrix, altering its absolute density (78). Crystallinity also
 593 increases over time during degradative attack of the amorphous regions leading
 594 to an increase in density (79).

595 However, these processes, potentially responsible for the sinking of LDP debris,
 596 have been observed only in laboratory studies or, in situ, uniquely at the sea
 597 surface (21, 22, 23, 24), with the exception of the recent observation of LDP in
 598 marine snow (80). The presence of LDP at depth is hence poorly understood.
 599 To investigate this question, we used a drag model and the largest collection of
 600 Mediterranean LDP debris to date. We calculated the difference of density be-
 601 tween sinking LDP debris and seawater necessary to obtain a theoretical sinking
 602 speed SS_{DM} equal to $SS_{MAX}=7.8$ m/d. We obtained $\Delta\rho=0.025$ kg/m³. As
 603 seawater density increases with depth (using a conservative estimate, about 1
 604 kg/m³ every 100 m; de la Fuente et al., (81)) LDP debris should stop sinking
 605 after 2.5 m if its density does not increase meanwhile. Therefore, our results

606 suggest that the biological processes proposed by the aforementioned studies
607 (e.g. 20, 75, 76) occur also below the surface.

608 This conclusion is corroborated by the fact that currents, in the Mediterranean
609 Sea, seems unable to transport LDP debris at great depths. Indeed, Soto-
610 Navarro et al., (38) have shown that vertical currents redistribute plastic debris
611 mainly in the first 100 meters of the water column. Onink et al., (82) predicted
612 a transport to greater depths primarily due to internal tides, but only for a small
613 proportion of LDP debris (<1%). Tsiaras et al., (74) studied the water column
614 plastic concentration in some regions of the Mediterranean Sea, and found that
615 model predictions were orders of magnitude lower than observations. In addition,
616 de la Fuente et al., (81) argued that neither the vertical nor horizontal
617 currents affect the water column debris concentration in the Mediterranean Sea
618 significantly (see in particular their Figure 5). Fischer et al., (70) suggested a
619 larger impact of vertical transport, but only when associated with an intense
620 biological activity.

621 All in all, our results point to the fact that LDP debris may persist in the wa-
622 ter column for time windows larger than previously suspected (e.g. 27, 16) and
623 travels for hundreds of kilometers. This can increase their bioavailability and
624 their potential negative impact for marine biota (3, 83). This study provides
625 an upper limit for the LDP sinking speed that can be used to constrain fu-
626 ture plastic-tracking studies. Further information on concentration of LDP in
627 the water column and on the seafloor, as well as observations of in situ sink-
628 ing speeds are urgently needed, given the potential damage of plastic debris on
629 pelagic and benthic ecosystems.

630 **4.4 Limits and perspectives**

631 The Lagrangian simulations were subject to approximations. We used a con-
632 stant sinking velocity of LDP particles from the surface to 1000 m depth, while
633 this can vary, due to seawater density variation or biochemical processes. The
634 sinking speed was considered equal for all the particles, while this may not be
635 the case (Subsec. 2.5). We focused on the 1000 m (and 2000 m, Supporting
636 Information S.2) depth layer, while several Mediterranean areas are deeper than
637 3000 m. Particles were released for one year only, and land based and maritime
638 plastic sources used to calculate the surface sinking rate (our initial condition)
639 were subject to high uncertainties (12, 27, 31). The surface sinking rate needs
640 further refinement, including processes such as fragmentation, seasonality and
641 spatial variability (e.g. 82). The horizontal and vertical diffusivity were consid-
642 ered as homogeneous through the basin and constant in time, while they can
643 have both spatial and temporal variability. These choices were due to the fact
644 that information about concrete ways of parameterising these dynamics (e.g.
645 the change in time of the sinking speed) were not available or not validated by
646 observations to date.

647 Therefore, while the concentration of LDPs on the seafloor is affected by high
648 uncertainties, our results represent a first step forward in the modelisation of
649 sinking LDP debris, as evidenced also by the agreement with in situ seafloor
650 observations. The hotspots of plastic debris accumulation on the seafloor as well
651 as its transport pathways may be used to design optimal sampling or removal
652 strategies (e.g. 31). These could be focused both at large or regional scales, and
653 may benefit from future improvements of TrackMPD simulated processes.

654 The previous considerations advocate for further research efforts, as additional
655 information is essential to deepen the knowledge on the biological processes
656 affecting the vertical path of plastic debris (e.g. refs. (32, 70, 74, 76)), and
657 to implement the characterisation of the hydrodynamical field transporting it
658 (for instance, by increasing its spatio-temporal resolution). Also, resuspension
659 from the seafloor or funnelling effects (for instance due to canyons) should be
660 investigated (16, 17, 84). This information is needed to improve plastic-tracking
661 models and, more generally, to mitigate plastic pollution.

662 Supporting Information

663 Use of individual sinking velocities and particle mass; LDP seafloor concentra-
664 tion at 2000 m; surface-seafloor connectivity; crossroadness analyses; sensitivity
665 test of SS_{DM} ; sensitivity test of LDP seafloor concentration; in situ obser-
666 vations of plastic seafloor concentration; sensitivity test of coastal strip LDP
667 concentration.

668 Acknowledgements

669 We thank the commitment of the following institutions: CNRS, Sorbonne Uni-
670 versity, LOV. The Tara Ocean Foundation and its founders and sponsors: agnès
671 b.®, Etienne Bourgois, the Veolia Environment Foundation, Lorient Agglom-
672 eration, Serge Ferrari, the Foundation Prince Albert II of Monaco, IDEC, the
673 “Tara” schooner, crews and teams. We thank MERCATOR-CORIOLIS and
674 ACRI-ST for providing daily satellite data during the expedition. We are also
675 grateful to the French Ministry of Foreign Affairs for supporting the expedi-
676 tion and to the countries that graciously granted sampling permission. The
677 authors are grateful to Enrico Ser-Giacomi for his helpful advice on the de-
678 sign of the research. We also thank Nicolas Benoit for continuous assistance
679 on the Mesu computational server, and Thomas Arsouze for the assistance on
680 the hydrodynamical product used. The authors thank Inés Jambou for her help
681 with the graphical abstract (Table of Contents graphic). This study is part
682 of the “PlastiMed BeMed : Closing the plastic tap” project conducted by the
683 International Union for Conservation of Nature (IUCN) with the financial sup-
684 port of the Prince Albert II of Monaco Foundation and EU H2020 LABPLAS
685 project under the grant agreement (ID: 101003954), DOI: 10.3030/101003954.
686 R.K. furthermore acknowledges support via a Make Our Planet Great Again
687 grant from the French National Research Agency (ANR) within the Programme
688 d’Investissements d’Avenir (reference ANR-19-MPGA-0012).

689 Data availability

690 All the data necessary to produce all the figures of the main text, including the
691 LDP seafloor concentration, the coastal strip pollution, and the SS_{DM} vs $\Delta\rho$
692 relationship, are publicly available at <https://doi.org/10.5281/zenodo.7350455>.
693 The surface sinking rate used to initialise the particle release is available at
694 <https://doi.org/10.5281/zenodo.5931213>. The in situ plastic concentrations are

⁶⁹⁵ available at <https://doi.org/10.5281/zenodo.5538237>. The TrackMPD code is
⁶⁹⁶ available at <https://github.com/IJalonRojas/TrackMPD>.

References

- 697
- 698 [1] David K. A. Barnes, Francois Galgani, Richard C. Thompson, and Morton
699 Barlaz, “Accumulation and fragmentation of plastic debris in global envi-
700 ronments”, *Philosophical Transactions of the Royal Society B: Biological*
701 *Sciences* **364**(1526), pp. 1985–1998 (2009).
- 702 [2] Nicola J. Beaumont, Margrethe Aanesen, Melanie C. Austen, Tobias Brger,
703 James R. Clark, Matthew Cole, Tara Hooper, Penelope K. Lindeque, Chris-
704 tine Pascoe, and Kayleigh J. Wyles, “Global ecological, social and economic
705 impacts of marine plastic”, *Marine Pollution Bulletin* **142**, pp. 189–195
706 (2019).
- 707 [3] Susanne Kühn and Jan Andries van Franeker, “Quantitative overview of
708 marine debris ingested by marine megafauna”, *Marine Pollution Bulletin*
709 **151**, pp. 110858 (2020).
- 710 [4] José Carlos García-Gómez, Marta Garrigós, and Javier Garrigós, “Plas-
711 tic as a vector of dispersion for marine species with invasive potential. a
712 review”, *Frontiers in Ecology and Evolution* **9** (2021).
- 713 [5] Charles Obinwanne Okoye, Charles Izuma Addey, Olayinka Oderinde,
714 Joseph Onyekwere Okoro, Jean Yves Uwamungu, Chukwudozie Kingsley
715 Ikechukwu, Emmanuel Sunday Okeke, Onome Ejeromedoghene, and Eli-
716 jah Chibueze Odii, “Toxic chemicals and persistent organic pollutants as-
717 sociated with micro-and nanoplastics pollution”, *Chemical Engineering*
718 *Journal Advances* **11**, pp. 100310 (2022).
- 719 [6] Anthony L. Andrady, “Microplastics in the marine environment”, *Marine*
720 *Pollution Bulletin* **62**(8), pp. 1596 – 1605 (2011).
- 721 [7] Atsuhiko Isobe, Takafumi Azuma, Muhammad Reza Cordova, Andrés
722 Cózar, Francois Galgani, Ryuichi Hagita, La Daana Kanhai, Keiri Imai,
723 Shinsuke Iwasaki, Shin’ichiro Kako, Nikolai Kozlovskii, Amy L. Lusher,
724 Sherri A. Mason, Yutaka Michida, Takahisa Mituhasi, Yasuhiro Morii,
725 Tohru Mukai, Anna Popova, Kenichi Shimizu, Tadashi Tokai, Keiichi
726 Uchida, Mitsuharu Yagi, and Weiwei Zhang, “A multilevel dataset of mi-
727 croplastic abundance in the world’s upper ocean and the Laurentian Great
728 Lakes”, *Microplastics and Nanoplastics* **1**(1), pp. 16 (2021).
- 729 [8] Jenna R. Jambeck, Roland Geyer, Chris Wilcox, Theodore R. Siegler,
730 Miriam Perryman, Anthony Andrady, Ramani Narayan, and Kara Laven-
731 der Law, “Plastic waste inputs from land into the ocean”, *Science*
732 **347**(6223), pp. 768–771 (2015).
- 733 [9] Erik Van Sebille, Chris Wilcox, Laurent Lebreton, Nikolai Maximenko,
734 Britta Denise Hardesty, Jan A Van Franeker, Marcus Eriksen, David Siegel,
735 Francois Galgani, and Kara Lavender Law, “A global inventory of small
736 floating plastic debris”, *Environmental Research Letters* **10**(12), pp. 124006
737 (2015).
- 738 [10] Winnie W. Y. Lau, Yonathan Shiran, Richard M. Bailey, Ed Cook, Mar-
739 tin R. Stuchtey, Julia Koskella, Costas A. Velis, Linda Godfrey, Julien

- 740 Boucher, Margaret B. Murphy, Richard C. Thompson, Emilia Jankowska,
741 Arturo Castillo Castillo, Toby D. Pilditch, Ben Dixon, Laura Koerselman,
742 Edward Kosior, Enzo Favoino, Jutta Gutberlet, Sarah Baulch, Meera E.
743 Atreya, David Fischer, Kevin K. He, Milan M. Petit, U. Rashid Sumaila,
744 Emily Neil, Mark V. Bernhofen, Keith Lawrence, and James E. Palardy,
745 “Evaluating scenarios toward zero plastic pollution”, *Science* **369**(6510),
746 pp. 1455–1461 (2020).
- 747 [11] Stephanie B. Borrelle, Jeremy Ringma, Kara Lavender Law, Cole C. Mon-
748 nahan, Laurent Lebreton, Alexis McGivern, Erin Murphy, Jenna Jambeck,
749 George H. Leonard, Michelle A. Hilleary, Marcus Eriksen, Hugh P. Possing-
750 ham, Hannah De Frond, Leah R. Gerber, Beth Polidoro, Akbar Tahir, Mi-
751 randa Bernard, Nicholas Mallos, Megan Barnes, and Chelsea M. Rochman,
752 “Predicted growth in plastic waste exceeds efforts to mitigate plastic pol-
753 lution”, *Science* **369**(6510), pp. 1515–1518 (2020).
- 754 [12] Lisa Weiss, Wolfgang Ludwig, Serge Heussner, Miquel Canals, Jean-Francois
755 Ghiglione, Claude Estournel, Mel Constant, and Philippe Kerhervé, “The
756 missing ocean plastic sink: Gone with the rivers”, *Science* **373**(6550), pp.
757 107–111 (2021).
- 758 [13] C. Anela Choy, Bruce H. Robison, Tyler O. Gagne, Benjamin Erwin,
759 Evan Firl, Rolf U. Halden, J. Andrew Hamilton, Kakani Katija, Susan E.
760 Lisin, Charles Rolsky, and Kyle S. Van Houtan, “The vertical distribution
761 and biological transport of marine microplastics across the epipelagic and
762 mesopelagic water column”, *Scientific Reports* **9**(1), pp. 7843 (2019).
- 763 [14] Matthias Egger, Fatimah Sulu-Gambari, and Laurent Lebreton, “First
764 evidence of plastic fallout from the North Pacific Garbage Patch”, *Scientific*
765 *Reports* **10**(1), pp. 7495 (2020).
- 766 [15] Charlotte Lefebvre, Claire Saraux, Olivier Heitz, Antoine Nowaczyk, and
767 Delphine Bonnet, “Microplastics ftir characterisation and distribution in
768 the water column and digestive tracts of small pelagic fish in the gulf of
769 lions”, *Marine Pollution Bulletin* **142**, pp. 510–519 (2019).
- 770 [16] Ian A. Kane, Michael A. Clare, Elda Miramontes, Roy Wogelius, James J.
771 Rothwell, Pierre Garreau, and Florian Pohl, “Seafloor microplastic
772 hotspots controlled by deep-sea circulation”, *Science* **368**(6495), pp. 1140–
773 1145 (2020).
- 774 [17] Martina Pierdomenico, Daniele Casalbore, and Francesco Latino Chiocci,
775 “Massive benthic litter funnelled to deep sea by flash-flood generated hy-
776 perpycnal flows”, *Scientific Reports* **9**(1), pp. 5330 (2019).
- 777 [18] F Galgani, J.P Leaute, P Moguedet, A Souplet, Y Verin, A Carpentier,
778 H Goragner, D Latrouite, B Andral, Y Cadiou, J.C Mahe, J.C Poulard,
779 and P Nerisson, “Litter on the Sea Floor Along European Coasts”, *Marine*
780 *Pollution Bulletin* **40**(6), pp. 516 – 527 (2000).
- 781 [19] I. Chubarenko, A. Bagaev, M. Zobkov, and E. Esiukova, “On some physical
782 and dynamical properties of microplastic particles in marine environment”,
783 *Marine Pollution Bulletin* **108**(1), pp. 105–112 (2016).

- 784 [20] Merel Kooi, Egbert H. van Nes, Marten Scheffer, and Albert A. Koelmans,
785 “Ups and downs in the ocean: Effects of biofouling on vertical transport
786 of microplastics”, *Environmental Science & Technology* **51**(14), pp. 7963–
787 7971 (2017).
- 788 [21] Francesca M.C. Fazey and Peter G. Ryan, “Biofouling on buoyant marine
789 plastics: An experimental study into the effect of size on surface longevity”,
790 *Environmental Pollution* **210**, pp. 354–360 (2016).
- 791 [22] David Kaiser, Nicole Kowalski, and Joanna J Waniek, “Effects of biofouling
792 on the sinking behavior of microplastics”, *Environmental Research Letters*
793 **12**(12), pp. 124003 (2017).
- 794 [23] Jan Gerritse, Heather A. Leslie, Caroline A. de Tender, Lisa I. Devriese,
795 and A. Dick Vethaak, “Fragmentation of plastic objects in a laboratory
796 seawater microcosm”, *Scientific Reports* **10**(1), pp. 10945 (2020).
- 797 [24] Katerina Karkanorachaki, Evdokia Syranidou, and Nicolas Kalogerakis,
798 “Sinking characteristics of microplastics in the marine environment”, *Sci-
799 ence of The Total Environment* **793**, pp. 148526 (2021).
- 800 [25] Matthew Cole, Penelope K. Lindeque, Elaine Fileman, James Clark, Ceri
801 Lewis, Claudia Halsband, and Tamara S. Galloway, “Microplastics alter the
802 properties and sinking rates of zooplankton faecal pellets”, *Environmental
803 Science & Technology* **50**(6), pp. 3239–3246 (2016), PMID: 26905979.
- 804 [26] Adam Porter, Brett P. Lyons, Tamara S. Galloway, and Ceri Lewis, “Role
805 of marine snows in microplastic fate and bioavailability”, *Environmental
806 Science & Technology* **52**(12), pp. 7111–7119 (2018), PMID: 29782157.
- 807 [27] S. Liubartseva, G. Coppini, R. Lecci, and E. Clementi, “Tracking plastics
808 in the Mediterranean: 2D Lagrangian model”, *Marine Pollution Bulletin*
809 **129**(1), pp. 151 – 162 (2018).
- 810 [28] Maria Luiza Pedrotti, Fabien Lombard, Alberto Baudena, Francois Galgani,
811 Amanda Elineau, Stephanie Petit, Maryvonne Henry, Romain Troublé,
812 Gilles Reverdin, Enrico Ser-Giacomi, Mikal Kedzierski, Emmanuel Boss,
813 and Gabriel Gorsky, “An integrative assessment of the plastic debris load
814 in the mediterranean sea”, *Science of The Total Environment* **838**, pp.
815 155958 (2022).
- 816 [29] Mikal Kedzierski, Maiaalen Palazot, Lata Soccalingame, Mathilde Falcou-
817 Prfol, Gabriel Gorsky, Francois Galgani, Stphane Bruzaud, and Maria Luiza
818 Pedrotti, “Chemical composition of microplastics floating on the surface
819 of the Mediterranean Sea”, *Marine Pollution Bulletin* **174**, pp. 113284
820 (2022).
- 821 [30] Roland Geyer, Jenna R. Jambeck, and Kara Lavender Law, “Production,
822 use, and fate of all plastics ever made”, *Science Advances* **3**(7) (2017).
- 823 [31] Alberto Baudena, Enrico Ser-Giacomi, Isabel Jalón-Rojas, François Gal-
824 gani, and Maria Luiza Pedrotti, “The streaming of plastic in the Mediter-
825 ranean Sea”, *Nature Communications* **13**(1), pp. 2981 (2022).

- 826 [32] Delphine Lobelle, Merel Kooi, Albert A. Koelmans, Charlotte Laufkter,
827 Cleo E. Jongedijk, Christian Kehl, and Erik van Sebille, “Global modeled
828 sinking characteristics of biofouled microplastic”, *Journal of Geophysical
829 Research: Oceans* **126**(4), pp. e2020JC017098 (2021), e2020JC017098
830 2020JC017098.
- 831 [33] Isabel Jalón-Rojas, Alicia Romero-Ramírez, Kelly Fauquembergue, Linda
832 Rossignol, Jérme Cachot, Damien Sous, and Bénédicte Morin, “Effects of
833 biofilms and particle physical properties on the rising and settling velocities
834 of microplastic fibers and sheets”, *Environmental Science & Technology*
835 **56**(12), pp. 8114–8123 (2022), PMID: 35593651.
- 836 [34] Andrés Cózar, Marina Sanz-Martín, Elisa Martí, J. Ignacio González-
837 Gordillo, Bárbara Ubeda, José á. Gálvez, Xabier Irigoien, and Carlos M.
838 Duarte, “Plastic accumulation in the Mediterranean Sea”, *PLOS ONE*
839 **10**(4), pp. 1–12 (2015).
- 840 [35] J. Mansui, G. Darmon, T. Ballerini, O. van Canneyt, Y. Ourmieres, and
841 C. Miaud, “Predicting marine litter accumulation patterns in the mediter-
842 ranean basin: Spatio-temporal variability and comparison with empirical
843 data”, *Progress in Oceanography* **182**, pp. 102268 (2020).
- 844 [36] Isabel Jalón-Rojas, Xiao Hua Wang, and Erick Fredj, “A 3D numerical
845 model to Track Marine Plastic Debris (TrackMPD): Sensitivity of mi-
846 croplastic trajectories and fates to particle dynamical properties and phys-
847 ical processes”, *Marine Pollution Bulletin* **141**, pp. 256 – 272 (2019).
- 848 [37] Thomas Arsouze, Jonathan Beuvier, Karine Béranger, Samuel Somot,
849 C Lebeauin Brossier, Romain Bourdallé-Badie, and Y Drillet, “Sensi-
850 bility analysis of the Western Mediterranean Transition inferred by four
851 companion simulations”, *CIESM, Marseille, France* **27** (2013).
- 852 [38] Javier Soto-Navarro, Gabriel Jordá, Salud Deudero, Carme Alomar, Ángel
853 Amores, and Montserrat Compa, “3d hotspots of marine litter in the
854 mediterranean: A modeling study”, *Marine Pollution Bulletin* **155**, pp.
855 111159 (2020).
- 856 [39] Victor Onink, David Wichmann, Philippe Delandmeter, and Erik van Se-
857 bille, “The role of Ekman currents, geostrophy, and Stokes drift in the
858 accumulation of floating microplastic”, *Journal of Geophysical Research:
859 Oceans* **124**(3), pp. 1474–1490 (2019).
- 860 [40] Kai Liu, Winnie Courtene-Jones, Xiaohui Wang, Zhangyu Song, Nian Wei,
861 and Daoji Li, “Elucidating the vertical transport of microplastics in the
862 water column: A review of sampling methodologies and distributions”,
863 *Water Research* **186**, pp. 116403 (2020).
- 864 [41] G.L. Lattin, C.J. Moore, A.F. Zellers, S.L. Moore, and S.B. Weisberg, “A
865 comparison of neustonic plastic and zooplankton at different depths near
866 the southern California shore”, *Marine Pollution Bulletin* **49**(4), pp. 291–
867 294 (2004).

- 868 [42] Katsiaryna Pabortsava and Richard S. Lampitt, “High concentrations of
869 plastic hidden beneath the surface of the Atlantic Ocean”, *Nature Com-
870 munications* **11**(1), pp. 4073 (2020).
- 871 [43] Matteo Baini, Maria Cristina Fossi, Matteo Galli, Iliana Caliani, Tommaso
872 Campani, Maria Grazia Finoia, and Cristina Panti, “Abundance and char-
873 acterization of microplastics in the coastal waters of tuscany (italy): The
874 application of the msfd monitoring protocol in the mediterranean sea”,
875 *Marine Pollution Bulletin* **133**, pp. 543–552 (2018).
- 876 [44] Grigoria Vasilopoulou, George Kehayias, Demetris Kletou, Periklis Kleitou,
877 Vassilios Triantafyllidis, Anastasios Zotos, Konstantinos Antoniadis, Maria
878 Rousou, Vassilis Papadopoulos, Polina Polykarpou, and George Tsiamis,
879 “Microplastics investigation using zooplankton samples from the coasts of
880 Cyprus (Eastern Mediterranean)”, *Water* **13**(16) (2021).
- 881 [45] Beatriz Rios-Fuster, Montserrat Compa, Carme Alomar, Valentina Fa-
882 giano, Ana Ventero, Magdalena Iglesias, and Salud Deudero, “Ubiquitous
883 vertical distribution of microfibers within the upper epipelagic layer of the
884 western mediterranean sea”, *Estuarine, Coastal and Shelf Science* **266**, pp.
885 107741 (2022).
- 886 [46] Kai Liu, Feng Zhang, Zhangyu Song, Changxing Zong, Nian Wei, and Daoji
887 Li, “A novel method enabling the accurate quantification of microplastics
888 in the water column of deep ocean”, *Marine Pollution Bulletin* **146**, pp.
889 462–465 (2019).
- 890 [47] Daoji Li, Kai Liu, Changjun Li, Guyu Peng, Anthony L. Andrady, Tianning
891 Wu, Zhiwei Zhang, Xiaohui Wang, Zhangyu Song, Changxing Zong, Feng
892 Zhang, Nian Wei, Mengyu Bai, Lixin Zhu, Jiayi Xu, Hui Wu, Lu Wang,
893 Siyuan Chang, and Wenxi Zhu, “Profiling the vertical transport of mi-
894 croplastics in the West Pacific Ocean and the East Indian Ocean with a
895 novel in situ filtration technique”, *Environmental Science & Technology*
896 **54**(20), pp. 12979–12988 (2020).
- 897 [48] La Daana K. Kanhai, Katarina Grdfeldt, Olga Lyashevskaya, Martin Has-
898 sellv, Richard C. Thompson, and Ian O’Connor, “Microplastics in sub-
899 surface waters of the Arctic Central Basin”, *Marine Pollution Bulletin* **130**,
900 pp. 8–18 (2018).
- 901 [49] X. Peng, M. Chen, S. Chen, S. Dasgupta, H. Xu, K. Ta, M. Du, J. Li,
902 Z. Guo, and S. Bai, “Microplastics contaminate the deepest part of the
903 world’s ocean”, *Geochemical Perspectives Letters* **9**, pp. 1–5 (2018).
- 904 [50] A. Bagaev, A. Mizyuk, L. Khatmullina, I. Isachenko, and I. Chubarenko,
905 “Anthropogenic fibres in the Baltic Sea water column: Field data, labora-
906 tory and numerical testing of their motion”, *Science of The Total Envi-
907 ronment* **599-600**, pp. 560–571 (2017).
- 908 [51] M R Cordova and U E Hernawan, “Microplastics in Sumba waters, East
909 Nusa Tenggara”, *IOP Conference Series: Earth and Environmental Science*
910 **162**, pp. 012023 (2018).

- 911 [52] Elena Gorokhova, “Screening for microplastic particles in plankton sam-
912 ples: How to integrate marine litter assessment into existing monitoring
913 programs?”, *Marine Pollution Bulletin* **99**(1), pp. 271–275 (2015).
- 914 [53] Miriam C. Goldstein, Andrew J. Titmus, and Michael Ford, “Scales of spa-
915 tial heterogeneity of plastic marine debris in the northeast pacific ocean”,
916 *PLOS ONE* **8**(11), pp. 1–11 (2013).
- 917 [54] M.B. Zobkov, E.E. Esiukova, A.Y. Zyubin, and I.G. Samusev, “Microplas-
918 tic content variation in water column: The observations employing a novel
919 sampling tool in stratified Baltic Sea”, *Marine Pollution Bulletin* **138**, pp.
920 193–205 (2019).
- 921 [55] Young Kyoung Song, Sang Hee Hong, Soeun Eo, Mi Jang, Gi Myung Han,
922 Atsuhiko Isobe, and Won Joon Shim, “Horizontal and Vertical Distribution
923 of Microplastics in Korean Coastal Waters”, *Environmental Science &
924 Technology* **52**(21), pp. 12188–12197 (2018).
- 925 [56] Mine B. Tekman, Claudia Wekerle, Claudia Lorenz, Sebastian Pimpke,
926 Christiane Hasemann, Gunnar Gerdt, and Melanie Bergmann, “Tying up
927 loose ends of microplastic pollution in the Arctic: Distribution from the
928 sea surface through the water column to deep-sea sediments at the HAUS-
929 GARTEN Observatory”, *Environmental Science & Technology* **54**(7), pp.
930 4079–4090 (2020), PMID: 32142614.
- 931 [57] Shiye Zhao, Erik R. Zettler, Ryan P. Bos, Peigen Lin, Linda A. Amaral-
932 Zettler, and Tracy J. Mincer, “Large quantities of small microplastics
933 permeate the surface ocean to abyssal depths in the south atlantic gyre”,
934 *Global Change Biology* **28**(9), pp. 2991–3006 (2022).
- 935 [58] Mikael L. A. Kaandorp, Henk A. Dijkstra, and Erik van Sebille, “Closing
936 the Mediterranean marine floating plastic mass budget: Inverse modeling
937 of sources and sinks”, *Environmental Science & Technology* **54**(19), pp.
938 11980–11989 (2020), PMID: 32852202.
- 939 [59] Julien Boucher and Guillaume Billard, “The mediterranean: Mare plas-
940 ticum”, *Gland, Switzerland: IUCN. x* **62** (2020).
- 941 [60] Mita Drius, Lucia Bongiorno, Daniel Depellegrin, Stefano Menegon,
942 Alessandra Pugnetti, and Simon Stifter, “Tackling challenges for Mediter-
943 ranean sustainable coastal tourism: An ecosystem service perspective”,
944 *Science of The Total Environment* **652**, pp. 1302–1317 (2019).
- 945 [61] Beatriz Morales-Nin, Antoni M. Grau, and Miquel Palmer, “Managing
946 coastal zone fisheries: A Mediterranean case study”, *Ocean & Coastal
947 Management* **53**(3), pp. 99–106 (2010).
- 948 [62] AJ Florczyk, M Melchiorri, C Corbane, M Schiavina, M Maffenini, M Pe-
949 saresi, P Politis, S Sabo, S Freire, D Ehrlich, T Kemper, P Tommasi,
950 D Airaghi, and L Zanchetta, “Description of the GHS Urban Centre
951 Database 2015”, *GHS Urban Centre Database 2015, multitemporal and
952 multidimensional attributes. European Commission, Joint Research Centre
953 (JRC)* (2019).

- 954 [63] Laurent C. M. Lebreton, Joost van der Zwet, Jan-Willem Damsteeg, Boyan
955 Slat, Anthony Andrady, and Julia Reisser, “River plastic emissions to the
956 world’s oceans”, *Nature Communications* **8**(1), pp. 15611 (2017).
- 957 [64] Lin Wu, Yongjun Xu, Qi Wang, Fei Wang, and Zhiwei Xu, “Mapping
958 global shipping density from AIS Data”, *Journal of Navigation* **70**(1), pp.
959 6781 (2017).
- 960 [65] Enrico Ser-Giacomi, Vincent Rossi, Cristóbal López, and Emilio
961 Hernández-García, “Flow networks: A characterization of geophysical
962 fluid transport”, *Chaos: An Interdisciplinary Journal of Nonlinear Sci-
963 ence* **25**(3), pp. 036404 (2015).
- 964 [66] Alberto Baudena, Enrico Ser-Giacomi, Cristóbal López, Emilio Hernández-
965 García, and Francesco d’Ovidio, “Crossroads of the mesoscale circulation”,
966 *Journal of Marine Systems* **192**, pp. 1 – 14 (2019).
- 967 [67] F. Dioguardi, D. Mele, and P. Dellino, “A new one-equation model of fluid
968 drag for irregularly shaped particles valid over a wide range of reynolds
969 number”, *Journal of Geophysical Research: Solid Earth* **123**(1), pp. 144–
970 156 (2018).
- 971 [68] Michiel Van Melkebeke, Colin Janssen, and Steven De Meester, “Character-
972 istics and sinking behavior of typical microplastics including the potential
973 effect of biofouling: Implications for remediation”, *Environmental Science
974 & Technology* **54**(14), pp. 8668–8680 (2020), PMID: 32551546.
- 975 [69] I. Jalón-Rojas, X.-H. Wang, and E. Fredj, “Technical note: On the im-
976 portance of a three-dimensional approach for modelling the transport of
977 neustic microplastics”, *Ocean Science* **15**(3), pp. 717–724 (2019).
- 978 [70] R. Fischer, D. Lobelle, M. Kooi, A. Koelmans, V. Onink, C. Laufkötter,
979 L. Amaral-Zettler, A. Yool, and E. van Sebille, “Modeling submerged bio-
980 fouled microplastics and their vertical trajectories”, *Biogeosciences Dis-
981 cussions* **2021**, pp. 1–29 (2021).
- 982 [71] Enrico Ser-Giacomi, Alberto Baudena, Vincent Rossi, Mick Follows, Sophie
983 Clayton, Ruggero Vasile, Cristóbal López, and Emilio Hernández-García,
984 “Lagrangian betweenness as a measure of bottlenecks in dynamical systems
985 with oceanographic examples”, *Nature Communications* **12**(1), pp. 4935
986 (2021).
- 987 [72] Julia Reisser, Maira Proietti, Jeremy Shaw, and Charitha Pattiaratchi,
988 “Ingestion of plastics at sea: does debris size really matter?”, *Frontiers in
989 Marine Science* **1** (2014).
- 990 [73] Amanda L. Dawson, So Kawaguchi, Catherine K. King, Kathy A.
991 Townsend, Robert King, Wilhelmina M. Huston, and Susan M. Bengt-
992 son Nash, “Turning microplastics into nanoplastics through digestive frag-
993 mentation by antarctic krill”, *Nature Communications* **9**(1), pp. 1001
994 (2018).

- 995 [74] Kostas Tsiaras, Yannis Hatzonikolakis, Sofia Kalaroni, Annika Pollani, and
 996 George Triantafyllou, “Modeling the pathways and accumulation patterns
 997 of micro- and macro-plastics in the Mediterranean”, *Frontiers in Marine
 998 Science* **8** (2021).
- 999 [75] Karin F. Kvale, A. E. Friederike Prowe, and Andreas Oschlies, “A critical
 1000 examination of the role of marine snow and zooplankton fecal pellets in
 1001 removing ocean surface microplastic”, *Frontiers in Marine Science* **6**, pp.
 1002 808 (2020).
- 1003 [76] K. Kvale, A. E. F. Prowe, C.-T. Chien, A. Landolfi, and A. Oschlies, “The
 1004 global biological microplastic particle sink”, *Scientific Reports* **10**(1), pp.
 1005 16670 (2020).
- 1006 [77] Jefferson T. Turner, “Zooplankton fecal pellets, marine snow, phytodetritus
 1007 and the oceans biological pump”, *Progress in Oceanography* **130**, pp. 205–
 1008 248 (2015).
- 1009 [78] Annika Jahnke, Hans Peter H. Arp, Beate I. Escher, Berit Gewert,
 1010 Elena Gorokhova, Dana Khnel, Martin Ogonowski, Annegret Potthoff,
 1011 Christoph Rummel, Mechthild Schmitt-Jansen, Erik Toorman, and
 1012 Matthew MacLeod, “Reducing uncertainty and confronting ignorance
 1013 about the possible impacts of weathering plastic in the marine environ-
 1014 ment”, *Environmental Science & Technology Letters* **4**(3), pp. 85–90 (2017).
- 1015 [79] M. J. Jenkins and K. L. Harrison, “The effect of crystalline morphology
 1016 on the degradation of polycaprolactone in a solution of phosphate buffer
 1017 and lipase”, *Polymers for Advanced Technologies* **19**(12), pp. 1901–1906
 1018 (2008).
- 1019 [80] Luisa Galgani, Isabel Gomann, Barbara Scholz-Bttcher, Xiangtao Jiang,
 1020 Zhanfei Liu, Lindsay Scheidemann, Cathleen Schlundt, and Anja Engel,
 1021 “Hitchhiking into the Deep: How Microplastic Particles are Exported
 1022 through the Biological Carbon Pump in the North Atlantic Ocean”, *Envi-
 1023 ronmental Science & Technology* **0**(0), pp. null (2022), PMID: 36302504.
- 1024 [81] R. de la Fuente, G. Drótos, E. Hernández-García, C. López, and E. van
 1025 Sebille, “Sinking microplastics in the water column: simulations in the
 1026 Mediterranean Sea”, *Ocean Science* **17**(2), pp. 431–453 (2021).
- 1027 [82] Victor Onink, Mikael L. A. Kaandorp, Erik van Sebille, and Charlotte
 1028 Laufketter, “Influence of Particle Size and Fragmentation on Large-Scale
 1029 Microplastic Transport in the Mediterranean Sea”, *Environmental Science
 1030 & Technology* **0**(0), pp. null (2022), PMID: 36270631.
- 1031 [83] S. Fabri-Ruiz, A. Baudena, F. Moullec, F. Lombard, J.-O. Irisson, and M.L.
 1032 Pedrotti, “Mistaking plastic for zooplankton: Risk assessment of plastic
 1033 ingestion in the mediterranean sea”, *Science of The Total Environment*
 1034 **856**, pp. 159011 (2023).
- 1035 [84] A. Ballent, S. Pando, A. Purser, M. F. Juliano, and L. Thomsen, “Modelled
 1036 transport of benthic marine microplastic pollution in the Nazaré Canyon”,
 1037 *Biogeosciences* **10**(12), pp. 7957–7970 (2013).